

# Age-Related Susceptibility to Apoptosis in Human Retinal Pigment Epithelial Cells Is Triggered by Disruption of p53–Mdm2 Association

Sujoy Bhattacharya,<sup>1</sup> Edward Chaum,<sup>2</sup> Dianna A. Johnson,<sup>2</sup> and Leonard R. Johnson<sup>1</sup>

**PURPOSE.** Relatively little is known about the contribution of p53/Mdm2 pathway in apoptosis of retinal pigment epithelial (RPE) cells or its possible link to dysfunction of aging RPE or to related blinding disorders such as age-related macular degeneration (AMD).

**METHODS.** Age-associated changes in p53 activation were evaluated in primary RPE cultures from human donor eyes of various ages. Apoptosis was evaluated by activation of caspases and DNA fragmentation. Gene-specific small interfering RNA was used to knock down expression of p53.

**RESULTS.** We observed that the basal rate of p53-dependent apoptosis increased in an age-dependent manner in human RPE. The age-dependent increase in apoptosis was linked to alterations in several aspects of the p53 pathway. p53 phosphorylation Ser15 was increased through the stimulation of ATM-Ser1981. p53 acetylation Lys379 was increased through the inhibition of SIRT1/2. These two posttranslational modifications of p53 blocked the sequestration of p53 by Mdm2, thus resulting in an increase in free p53 and of p53 stimulation of apoptosis through increased expression of PUMA (p53 upregulated modulator of apoptosis) and activation of caspase-3. Aged RPE also had reduced expression of antiapoptotic Bcl-2, which contributed to the increase in apoptosis. Of particular interest in these studies was that pharmacologic treatments to block p53 phosphorylation, acetylation, or expression were able to protect RPE cells from apoptosis.

**CONCLUSIONS.** Our studies suggest that aging in the RPE leads to alterations of specific checkpoints in the apoptotic pathway, which may represent important molecular targets for the treatment of RPE-related aging disorders such as AMD. (*Invest Ophthalmol Vis Sci.* 2012;53:8350–8366) DOI:10.1167/iov.12-10495

A major challenge in vision research is the identification of the causative factors that lead to declines in retinal function that will ultimately result in age-related macular degeneration (AMD) for a projected 3 million individuals in the United States with neovascular AMD and/or geographic atrophy by 2020.<sup>1</sup> One promising strategy in understanding this multifactorial disease process is to identify and track age-dependent changes in cellular pathways, especially in cells of the retinal pigment epithelium (RPE) because these represent the gatekeepers whose loss of functional integrity has been linked to retinal aging.<sup>2–4</sup> RPE cells constitute a major component of the blood-retinal barrier (BRB) and loss of integrity of tight junctions (TJs) and adherens junctions (AJs) in RPE can disrupt photoreceptor homeostasis.<sup>5–9</sup> RPE cells also phagocytose tips of outer segments normally shed by photoreceptors, generate melanosomes to function as a light and heat sink, provide trophic factors, and recycle visual pigments. Many of the hallmarks of AMD reflect malfunctions of these RPE-related pathways, including photobleaching of melanosomes, accumulation of lipofuscin granules, impairment of outer segment phagocytosis, formation of drusen, and breakdown of the BRB in advanced cases (neovascular AMD).<sup>5,9–14</sup>

Throughout life, the RPE is continuously challenged by high oxygen tension and exposure to photic stress, particularly in the macular region. These conditions are known to trigger apoptosis in other cell types, but normally the RPE appears to be resilient in part due to specific modifications of the apoptotic pathway. Our group<sup>15</sup> and others have shown that normal RPE has unusually low levels of caspase-8,<sup>16</sup> high levels of antiapoptotic Bcl-2 family proteins,<sup>15,17</sup> and neuroprotectin-D1,<sup>18</sup> all of which serve to inactivate proapoptotic and proinflammatory signaling pathways. We now seek to determine if these antiapoptotic conditions degrade during aging so that RPE cells become vulnerable to normal proapoptotic stressors, creating a tipping point beyond which retinal homeostasis is lost along with visual function.

Tumor suppressor p53 acts as a key trigger for the induction of apoptosis, or in some cases cell cycle arrest, in response to various stressors.<sup>19,20</sup> The availability of p53 is regulated by p53 binding proteins, Mdm2 and Mdm4 (also known as Mdmx), both of which bind and sequester p53.<sup>21,22</sup> It has been shown that binding of p53 to Mdm2 or Mdm4 promotes p53 ubiquitination and degradation, thus providing a negative autoregulatory mechanism of p53 stability and activity.<sup>21,23</sup> Nutlin-3, a synthetic small-molecule Mdm2 inhibitor, preferentially binds to the p53-binding pocket of Mdm2, disrupts p53–Mdm2 association, and effectively activates p53 in various cell types.<sup>24</sup> Using Nutlin-3 and other drugs, we have recently shown that destabilization of the p53–Mdm2 interaction is sufficient for the induction of apoptosis in primary RPE cultures.<sup>15</sup>

From the Departments of <sup>1</sup>Physiology and <sup>2</sup>Ophthalmology, University of Tennessee Health Science Center, Memphis, Tennessee.

Supported by William Webster Endowment Fund in Neurosciences Grant R073037299, National Institute of Diabetes and Digestive and Kidney Diseases Grant DK-16505, an unrestricted grant from Research to Prevent Blindness (New York, New York), and the Plough Foundation (Memphis, Tennessee). The authors alone are responsible for the content and writing of the paper.

Submitted for publication June 29, 2012; revised September 28 and October 30, 2012; accepted November 1, 2012.

Disclosure: **S. Bhattacharya**, None; **E. Chaum**, None; **D.A. Johnson**, None; **L.R. Johnson**, None

Corresponding author: Sujoy Bhattacharya, Department of Physiology, University of Tennessee Health Science Center, 894 Union Avenue, Memphis, TN 38163; sbhatta3@uthsc.edu.

Several studies have shown that posttranslational modifications of p53, including phosphorylation and acetylation, regulate p53-Mdm2 interaction and, consequently, affect p53 stability and activity.<sup>20,25</sup> Ataxia telangiectasia mutated and Rad3-related family kinases (ATM/ATR) are required for the rapid phosphorylation of p53 at Ser15 in response to DNA damage and replication stalling.<sup>26</sup> In addition, the Sir family of proteins (sirtuins: SIRT1–7) is a group of nicotinamide (NAD<sup>+</sup>)-dependent deacetylases/ADP-ribosyltransferases that catalyzes the deacetylation of p53 and modulates p53-dependent cell death.<sup>27,28</sup> Acetylation of p53 is believed to increase p53 stability by preventing ubiquitination and degradation.<sup>28</sup> Thus the activity of SIRT family proteins is inversely related to the rate of p53 acetylation, stabilization, and activation of apoptosis. SIRT family proteins are thought to act as metabolic master regulators of lifespan in mammals.<sup>29</sup> Despite the known involvement of SIR2 family proteins in several processes including metabolism, apoptosis, differentiation, and aging,<sup>30</sup> there is currently no evidence of involvement of these pathways in RPE apoptosis.

Emerging data indicate that the ubiquitin-proteasome pathway (UPP) is required for the transcriptional activation of p53.<sup>31</sup> The UPP is the major protein degradation pathway in the cell and is involved in the regulation of multiple cellular processes including cell cycle regulation, DNA repair,<sup>32</sup> and aging.<sup>33</sup> Although an age-related decrease in ubiquitin-proteasome activity has been reported, little information is available about the role of UPP during RPE aging. Given that RPE cells proliferate throughout life and aging decreases RPE proliferation and increases susceptibility to apoptosis, we hypothesized that age-related inhibition of UPP is mechanistically linked with p53 activation and RPE apoptosis.

p53 hyperactivity has been shown to correlate with aging in several mouse models. Heterozygous mice with constitutively active p53 and enhanced stability of the p53 protein have shorter lifespans with accelerated aging phenotypes.<sup>34</sup> Similarly, metalloproteinase (*Zmpste24*)-deficient mice exhibit accelerated aging and progeroid phenotypes due to marked upregulation of p53 signaling.<sup>35</sup> In a recent study, Abdouh et al.<sup>36</sup> demonstrated that inactivation of the Polycomb group gene *Bmi1* in mice resulted in premature aging-like phenotype due to upregulation of p53 activity.

Our current hypothesis is that age-related changes in the p53/Mdm2 pathway, including changes in p53 acetylation and phosphorylation, may underlie age-related degeneration in RPE cells and lead to loss of visual function in retinal neurons and eventually to AMD. Our studies suggest for the first time that age-related posttranslational modifications of p53 limit binding to Mdm2, which frees p53 to stimulate caspase-3, activate apoptosis, and thereby trigger the pathogenesis that could lead to AMD. Taken together, our findings identify important constituents of the p53/Mdm2 pathway that could serve as targets for treatment of the disease.

## MATERIALS AND METHODS

### Reagents

Disposable cell culture ware was purchased commercially (Corning Glass Works, Corning, NY; and Zellkulture Flaschen; Techno Plastic Products AG, Trasadingen, Switzerland). Cell culture medium and fetal bovine serum (FBS) were also obtained commercially (Mediatech, Inc., Herndon, VA; and Invitrogen, Long Island, NY), as were permeable supports (Transwell; Corning, Lowell, MA). Other materials, purchased commercially, were: enhanced chemiluminescence (ECL) Western blot detection system (PerkinElmer, Inc., Boston, MA); Phospho-p53 Ser15, Acetyl p53 Lys379, total-p53, cleaved active caspase-3 (Asp 175),

phospho-ATM Ser1981, total-ATM, phospho-Rb Ser780, and phospho-H2AX Ser139 antibodies (Cell Signaling Technology, Inc., Beverly, MA); p21Cip1 antibodies (BD Biosciences, San Diego, CA); Nutlin-3 (Sigma, St. Louis, MO); Sirtinol, Resveratrol, MG132, and CGK733 (EMD Biosciences/Millipore Corp., Billerica, MA); p53 small interfering (si)RNA, p53 (DO-1), p53-agarose conjugate, Mdm2 (SMP14), total-Rb, and Nucleolin specific antibodies (Santa Cruz Biotechnology, Santa Cruz, CA); Mdm4 antibody (Millipore Corp., Billerica, MA); Zonula Occludens (ZO-1) and beta-catenin antibodies (Zymed Laboratories Inc., South San Francisco, CA); Alexa-Fluor 488 conjugated and Cy3 conjugated secondary antibodies (Molecular Probes, Eugene, OR); cell death detection ELISA Plus kit (Roche Diagnostics Corp., Indianapolis, IN); mounting medium with 4',6-diamidino-2-phenylindole (DAPI; Vector Laboratories, Burlingame, CA). All chemicals were of the highest purity commercially available.

### Primary RPE Cell Culture

Primary human RPE cells were isolated from postmortem donor eyes provided by the Midsouth Eye Bank and National Disease Research Interchange (NDRI) using procedures previously described.<sup>37</sup> The Institutional Review Board at the University of Tennessee Health Science Center approved the use of human eyes from deidentified donors. Donor eyes were stratified into two cohorts: donors 40 years of age or less were classified as young, donors 65 years and older as aged. All postmortem donor eyes were shipped to our laboratory within 24 hours of enucleation. Three pairs of young donor eyes: 29, 40, and 41 years of age were used in our studies. In addition, aged donors 81, 84, 86, 90, and 94 years of age were used to study the effects of aging on RPE pathology. Inclusion criteria for aged donor eyes included the absence of diagnostic criteria for AMD from the postmortem metadata profile. These features were confirmed by microscopic examination of the postmortem retinas. Exclusion criteria of aged eyes included known retinal dystrophies, diabetic retinopathy, uveitis, trauma, prior retinal laser treatment, or other proliferative or degenerative retinal diseases. Globes were incised and the anterior segment was removed. The vitreous was extracted manually and the retina was dissected free. The eyecup was washed three times with Dulbecco's modified Eagle's medium (DMEM), and 0.25% trypsin/EDTA was applied for four 15-minute digestion cycles. Cells were loosened by aspiration. Finally, cells were transferred to DMEM with FBS. Cells were spun at 2000g for 5 minutes and the pellet was resuspended in DMEM with 15% FBS and plated in poly-L-lysine-coated 12-well cell culture ware. The fastest growing cells with cobblestone morphology were used for our studies. Primary cultures within the first three passages were used. Stock cells were grown in T-25 flasks in a humidified, 37°C incubator in an atmosphere of 5% CO<sub>2</sub>. Stock cells were maintained in cell culture medium consisting of DMEM and Ham's F12 medium (1:1 ratio) containing L-glutamine and 10% heat inactivated FBS. For experimental purposes, 0.75 × 10<sup>6</sup> cells were seeded per 60-mm plate so that cells were 90% confluent by day 3. RPE cells were grown in control medium and serum starved for 24 hours (to allow synchronization of the cell cycle), followed by the induction of apoptosis.

### Apoptosis

The quantitative DNA fragmentation assay was carried out using a cell death detection ELISA kit as described earlier (Roche Diagnostics Corp.).<sup>38–40</sup> An aliquot of nuclei-free cell lysate was placed in streptavidin-coated wells and incubated with anti-histone-biotin antibody and anti-DNA peroxidase conjugated antibody for 2 hours at room temperature. After incubation, the sample was removed and the wells were washed followed by incubation with 100 μL of the substrate (2,2'-azino-di[3-ethylbenzthiazolin-sulfonate]) and allowed to react at room temperature. The absorbance was read at 405 nm using a plate reader (Synergy HT; Bio-Tek Instruments, Inc., Winooski, VT). Results were expressed as absorbance at 405 nm/min/mg protein.

## Cell Proliferation

RPE cell proliferation was measured as described before.<sup>15</sup> Equal numbers of cells were plated in six-well plates. Cells were allowed to attach for 24 hours followed by treatment with 25  $\mu$ M Sirtinol, 5  $\mu$ M Nutlin-3, or DMSO (vehicle control) in serum-containing medium. Cells were trypsinized and counted after 48 hours of treatment.

## Transfection

RPE cells were seeded in six-well plates at a density of  $0.35 \times 10^6$  cells/well in antibiotic-free normal growth medium to achieve 60% to 70% confluence on day 2. Transfection of RPE cells was performed using protocols described previously.<sup>15</sup> Briefly, 2 to 8  $\mu$ L siRNA duplex (0.25–1  $\mu$ g) was diluted in 100  $\mu$ L DMEM without serum and antibiotics and labeled as A; 2 to 8  $\mu$ L FUGENE transfection reagent was diluted in serum-free medium and labeled as B. Solutions A and B were mixed together and incubated at room temperature for 30 to 45 minutes. The cell monolayer was rinsed in serum and antibiotic-free DMEM, and the siRNA-transfection mix was added dropwise to the monolayer and incubated for 12 hours at 37°C. Fresh medium containing serum and antibiotics was added to the monolayer without removing the transfection mixture and incubated for an additional 12 hours. The cells were serum starved and then treated with 60  $\mu$ M Nutlin-3. Total cell lysates were prepared for Western blotting.

## Detection of Apoptotic Cells by TUNEL Assay

TUNEL (terminal deoxynucleotide transferase-mediated dUTP nick end labeling) staining was performed using the fluorescein-based in situ cell death detection kit (Roche Diagnostics Corp.) according to the manufacturer's instructions. Primary RPE cultures were grown on biodegradable gelatinous protein mixture-coated coverslips (Matrigel; BD Biosciences, Franklin Lakes, NJ) and fixed in 3.7% paraformaldehyde for 20 minutes followed by permeabilization with 0.1% Triton X-100 (Bio-Rad Laboratories, Hercules, CA) in 0.1% citrate buffer for 7 minutes. Monolayers were washed with PBS and incubated with TUNEL mixture for 1 hour at room temperature. Finally, cells were washed with PBS, mounted on glass slides using mounting medium containing DAPI, and viewed using an image deconvolution system (Nikon Diaphot microscope; Nikon Instruments, Inc., Melville, NY). Images were analyzed with ImageJ software (developed by Wayne Rasband, National Institutes of Health, Bethesda, MD; available at <http://rsbweb.nih.gov/ij/index.html>) and processed by commercial image-editing software (Adobe Photoshop; Adobe Systems Inc., San Jose, CA).

## Western Blot Analysis

The protocol for Western blotting has been described earlier.<sup>38–40</sup> Typically, cell monolayers were first washed with ice-cold Dulbecco's PBS (DPBS) and lysed for 10 minutes in ice-cold cell lysis buffer containing protease inhibitors. Lysates were centrifuged at 10,000g for 10 minutes at 4°C followed by SDS-PAGE. Proteins were transferred to high-performing transfer membranes (Immobilon-P; Millipore, Bedford, MA) and probed with the indicated antibodies overnight at 4°C in TBS buffer containing 0.1% Tween-20 and 5% nonfat dry milk (blotting grade; Bio-Rad Laboratories). Membranes were subsequently incubated with horseradish peroxidase-conjugated secondary antibodies at room temperature for 1 hour, and the immunocomplexes were visualized by the ECL detection system (PerkinElmer, Inc.). Representative Western blots from three experiments are shown. Densitometric analysis of all Western blots was performed using ImageJ software (National Institutes of Health).

## Immunofluorescence Microscopy

RPE cell monolayers were cultured on inserts (Transwell) and fixed in ice-cold acetone/methanol (1:1) followed by permeabilization in 0.1% Triton X-100 (Bio-Rad Laboratories). After permeabilization, the monolayers were blocked in 5% BSA in PBS and further incubated with primary antibodies (rabbit polyclonal ZO-1, mouse beta-catenin, nucleolin, and mouse p53) for 1 hour at 37°C, followed by 1-hour incubation with secondary antibodies (Alexa Fluor 488-conjugated and Cy3-conjugated secondary antibodies [Molecular Probes]). The fluorescence was examined under a laser scanner confocal microscope (Zeiss LSM 5; Carl Zeiss AG, Oberkochen, Germany) and images were collected using a light microscopy software system (LSM 5 Pascal software; Carl Zeiss AG) as described earlier.<sup>41</sup> Images were stacked using ImageJ software (National Institutes of Health) and processed by commercial image-editing software (Adobe Photoshop; Adobe Systems Inc.).

## Statistical Analysis

All data are expressed as mean  $\pm$  SE. Experiments were repeated three times, with triplicate samples for each. Representative Western blots from three experiments are shown. ANOVA and appropriate post hoc testing determined the significance of the differences between means. Values of  $P < 0.05$  were considered significant.

## RESULTS

### Effect of Aging on Apoptosis and Junctional Integrity in Human RPE Cells

Accumulating evidence suggests that aging can both inhibit cell death leading to cancer, and potentiate cell death causing tissue atrophy.<sup>42</sup> Primary RPE cultures from young and aged donor eyes were grown to confluence and analyzed for active caspase-3 using specific antibody. Our data show increased levels of active caspase-3 in aged human RPE (Fig. 1A). In addition, aging significantly increased DNA fragmentation in human RPE (Fig. 1B). To confirm age-related apoptosis, cell monolayers were analyzed by TUNEL staining and mounted on slides using mounting medium containing DAPI, a fluorescent stain that binds to DNA. The appearance of TUNEL-positive cells (see arrowheads, Fig. 1C) indicates age-related induction of RPE apoptosis.

In addition to increases in TUNEL-positive cells, we observed other age-related differences that were concomitant with apoptosis, that is, a decrease in tight and adherens junctions, as assessed by the immunofluorescent localization of ZO-1, and beta-catenin using confocal microscopy. In confluent human RPE monolayers obtained from young donors, ZO-1 was localized in the periphery, indicating formation of tight junctions (Fig. 1D). Immunostaining for beta-catenin showed intense peripheral localization and some intracellular staining in young RPE cultures. Merged images indicate peripheral colocalization of ZO-1 and beta-catenin in the intercellular junctions. Aging induced discontinuities in the network of tight and adherens junctional strands and redistributed ZO-1 and beta-catenin from the intercellular junctions (Fig. 1D). Our results suggest that the normal aging process disrupts junctional integrity in human RPE.

### Epigenetic Modifications of p53 Cause Mitochondrial Dysfunction in Aged RPE

Since p53 is a molecular gatekeeper of apoptosis and cell cycle arrest in multiple cell types, and constitutive activation of p53 correlates with accelerated aging, we investigated whether



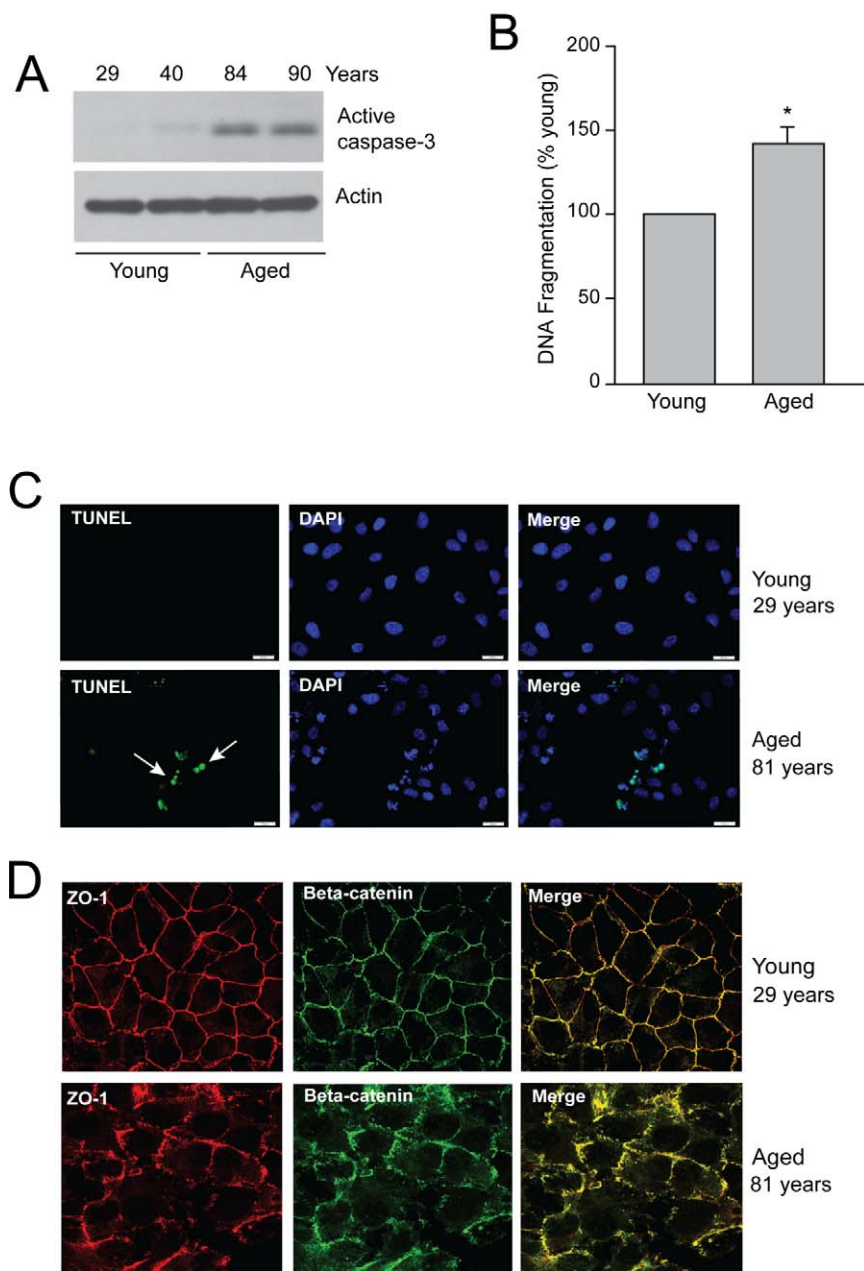


**FIGURE 1.** Aging induces apoptosis of RPE cells. RPE cells were isolated from young and aged donor eyes, and primary cultures were grown to confluence. **(A)** Cell lysates were separated on SDS-PAGE, and Western blot analysis was carried out using an antibody specific for active caspase-3. **(B)** DNA fragmentation was measured by ELISA (mean  $\pm$  SEM,  $n = 3$  from young [donor age 29, 40, and 41 years] and aged groups [donor age 81, 86, and 94 years]). \*, significantly different compared with young RPE cells ( $P < 0.05$ ). **(C)** Cell monolayers were analyzed by TUNEL staining using a kit from Roche and following the manufacturer's instructions. DAPI-containing mounting medium was used to stain nucleus. *Arrowheads* represent apoptotic cells. *Scale bar*, 20  $\mu$ m. **(D)** Age-related disruption of tight and adherens junctions in RPE cells. RPE cells were obtained from young and aged human eye donors. Primary cultures were grown to confluence and monolayers were fixed and stained for ZO-1 (red) and beta-catenin (green) by the immunofluorescence. Proteins were localized using confocal microscopy. *Scale bar*, 20  $\mu$ m.

increased levels of apoptosis in aged RPE cultures is concomitant with activation of p53. Primary RPE cultures from a cohort of young (Y1–Y3) and aged donors (A1–A5) (donor ages presented in Table 1) were analyzed for changes in p53 expression using Western blot analysis. Basal levels of p53 were low in young RPE cultures. By contrast, aged RPE showed increased expression of p53, which varied between different donors (Fig. 2A). In RPE cells obtained from young donors, low levels of phosphorylation at Ser15, acetylation at Lys379, and

expression of p53 were observed. Aging robustly increased p53 phosphorylation and acetylation (Figs. 2B, 2C), which were accompanied by significant increases of free p53 and Mdm2 protein. To investigate an independent marker of cellular aging, we further measured the protein level of endogenous CDK inhibitor p21Cip1, which is a transcriptional downstream target of p53. Increased expression of p21Cip1 is a well-known marker of replicative senescence<sup>43</sup> and has been demonstrated to be associated with stem-cell aging.<sup>44</sup> As

**TABLE 1.** Cohorts of Deidentified Young (Y) and Aged (A) Eye Donors and Their Respective Ages

List of Eye Donors	Donor Ages, y
Young-Y1	29
Young-Y2	40
Young-Y3	41
Aged-A1	81
Aged-A2	84
Aged-A3	86
Aged-A4	90
Aged-A5	94

shown in Figures 2B and 2C, increased expression of p21Cip1 was observed in aged RPE. Since DNA damage rapidly triggers phosphorylation of histone H2AX on Ser139,<sup>45</sup> and since H2AX is required for DNA fragmentation,<sup>46</sup> we measured age-related phosphorylation of H2AX. Endogenous levels of the phosphorylated H2AX ( $\gamma$ -H2AX) were low in RPE from young donors, whereas RPE from aged donors contained significantly higher levels of  $\gamma$ -H2AX, suggesting that DNA damage is associated with aging (Figs. 2B, 2C).

Under basal conditions, p53 is mainly localized in the cytoplasm. Several studies have shown that p53 undergoes modification in response to cellular stress and eventually translocates to the nucleus.<sup>47</sup> Nuclear translocation of p53 stimulates its sequence-specific DNA-binding activity.<sup>48</sup> Since the aging process modifies p53 (Figs. 2B, 2C), we investigated its subcellular localization in young and aged RPE cells. Young cells stained strongly for cytoplasmic p53 (Fig. 2D, green). However, p53 staining increased and was localized to bright nuclear foci in aged cells (Fig. 2D). To confirm nuclear translocation of p53, we immunostained RPE cells with both anti-p53 and anti-nucleolin antibodies. Nucleolin, a major nucleolar phosphoprotein, accumulates predominantly within the nucleolus by virtue of binding to nucleolar compartments, and is known to colocalize with p53.<sup>49</sup> p53 and nucleolin strongly colocalized (yellow) in the nucleus of RPE cells obtained from aged donors (Fig. 2D), further indicating that age-related modification of p53 may induce nucleolar localization.

RPE cells from young human donors expressed high levels of antiapoptotic Bcl-2 protein (Figs. 3A, 3B), which is consistent with our previous observations.<sup>15</sup> The aging process significantly decreased Bcl-2 expression (Figs. 3A, 3B). Furthermore, age-related modifications of p53 preferentially promoted transcription of its proapoptotic target p53 upregulated modulator of apoptosis (PUMA), which in turn significantly increased PUMA expression (Figs. 3A, 3B). Phosphorylation and/or acetylation of p53 disrupt its interactions with Mdm2, leading to p53 stabilization. Therefore, we investigated whether posttranslational modifications of p53 in aging RPE alter the association of p53 and Mdm2. RPE cell lysates obtained from young and aged donors were subjected to immunoprecipitation using p53 antibody and analyzed for the presence of Mdm2. Bound Mdm2 was detected in immune complexes from young RPE cells (Figs. 3C, 3D). However, immune complexes from aged RPE cells contained lesser amounts of Mdm2. These results suggest that epigenetic modifications of p53 disrupt this association (Figs. 3C, 3D) and thereby fail to keep p53 activation in check. In addition, Bcl-2 was detected in p53 immunoprecipitates from young RPE (Figs. 3C, 3D), suggesting that Bcl-2 interacts with p53 and negatively regulates its apoptotic activity. Immunoprecipitation of p53 in aged RPE brought down PUMA, but reduced levels of Bcl-2 were observed (Figs. 3C, 3D). These

results indicate that proapoptotic BH3 domain protein, PUMA, displaces Bcl-2 proteins from their association with p53 in aged RPE. Consequently, p53 complexes with PUMA causing mitochondrial dysfunction, eventually culminating in cell death.

### ATM/ATR Kinase Phosphorylates p53 in Response to Aging

ATM/ATR-dependent phosphorylation of p53 following DNA damage enhances p53 activity.<sup>50</sup> Our data show increased activation of ATM kinase via phosphorylation on Ser1981 in aged RPE cells (Figs. 4A, 4B). Increased phosphorylation of ATM/ATR kinase was concomitant with increased levels of p53 phosphorylation on Ser15 and apoptosis in aged RPE cells. To determine the contribution of ATM kinase in age-induced p53 phosphorylation, we treated young RPE cells with the ATM/ATR kinase inhibitor CGK733 followed by treatment with Nutlin-3. Consistent with our previous observations,<sup>15</sup> disruption of p53-Mdm2 interaction by Nutlin-3 significantly increased expression and phosphorylation of p53 on Ser15, which in turn caused caspase-3 activation and apoptosis in young RPE cells (Figs. 4C, 4D). Inhibition of ATM/ATR kinase blocked Nutlin-3-induced phosphorylation and expression of p53 and subsequently inhibited caspase-3 activation (Figs. 4C, 4D), suggesting a pivotal role of these kinases in mediating proapoptotic role of p53 in aged RPE. To further confirm that increased phosphorylation of p53 observed in aged RPE cells is dependent on ATM/ATR kinase, we treated aged RPE cells with CGK733. Increased phosphorylation of ATM Ser1981 normally seen in aged RPE cells (Figs. 4E, 4F) was blocked by CGK733, suggesting the effectiveness of the pharmacologic inhibitor. Treatment of aged RPE cells with CGK733 partially decreased ATM expression. Furthermore, CGK733 blocked phosphorylation of p53 Ser15, which in turn decreased stabilization of p53 and led to degradation. As a result, p53 expression decreased in aged RPE cells (Figs. 4E, 4F). These observations indicate that physiologic aging triggers p53 stabilization and activation through ATM.

### SIRT1/2 Inhibition by Sirtinol Induces RPE Apoptosis

Previous studies have shown that SIRT1 binds and deacetylates p53, leading to its inactivation.<sup>28</sup> To determine if inhibition of SIRT1 using Sirtinol caused p53 acetylation in RPE cells, young confluent quiescent RPE monolayers were treated with 50  $\mu$ M Sirtinol for 48 hours. Sirtinol increased the amount of acetylated p53 (Figs. 5A, 5B). Interestingly, inhibition of SIRT1 increased p53 phosphorylation but had a marginal effect on p53 expression (Figs. 5A, 5B), suggesting that acetylation of p53 (known to activate its function) may facilitate its ability to be phosphorylated. Activation of p53 in response to Sirtinol was concomitant with increased caspase-3 activation and apoptosis of young RPE cells, clearly suggesting that acetylation and phosphorylation of p53 seen in aged RPE cells contribute to apoptosis.

### Resveratrol Inhibits Nutlin-3-Induced RPE Apoptosis

Resveratrol, a polyphenol found in red wine, has been reported to act as a sirtuin activator and has gained significant attention for its antioxidative and antiaging effects.<sup>51</sup> To determine whether activation of SIRT1 increased deacetylation of p53 and consequently inhibited p53-dependent apoptosis, we treated young RPE cells with 25  $\mu$ M Resveratrol overnight followed by

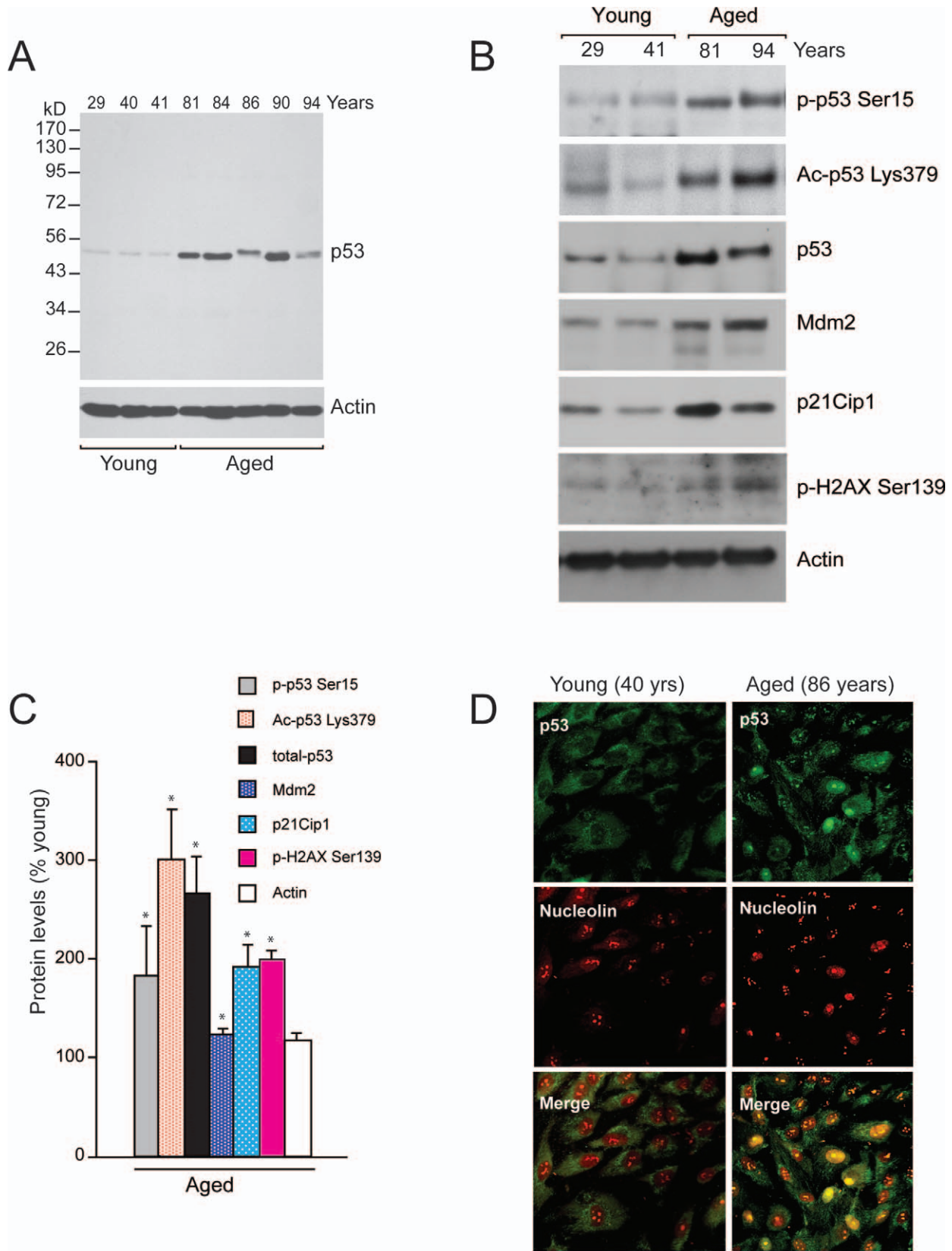


**FIGURE 2.** Age-induced posttranslational modification of p53. Primary cultures of RPE cells obtained from cohorts of young and aged donor eyes were grown to confluence. **(A)** RPE cell lysates were analyzed for p53 expression using specific antibody. Blot was stripped and probed for actin as an internal loading control. **(B)** Cell lysates were analyzed by Western blot for phospho Ser15, Acetyl-Lys389, and total-p53, Mdm2, p21Cip1, and phospho-H2AX Ser139 using specific antibodies. Actin was used as an internal loading control. **(C)** Densitometric analysis of results shown in **(A)**. Values from young RPE cells were set at 100%. \*, significantly different compared with young RPE cells ( $P < 0.05$ ). **(D)** Nuclear translocation of p53 in aged RPE cells. Confluent RPE monolayers were fixed and stained using antibodies specific for p53 (green) and nucleolin (red). Localization of proteins was carried out using confocal microscopy. Scale bar, 20  $\mu$ m.



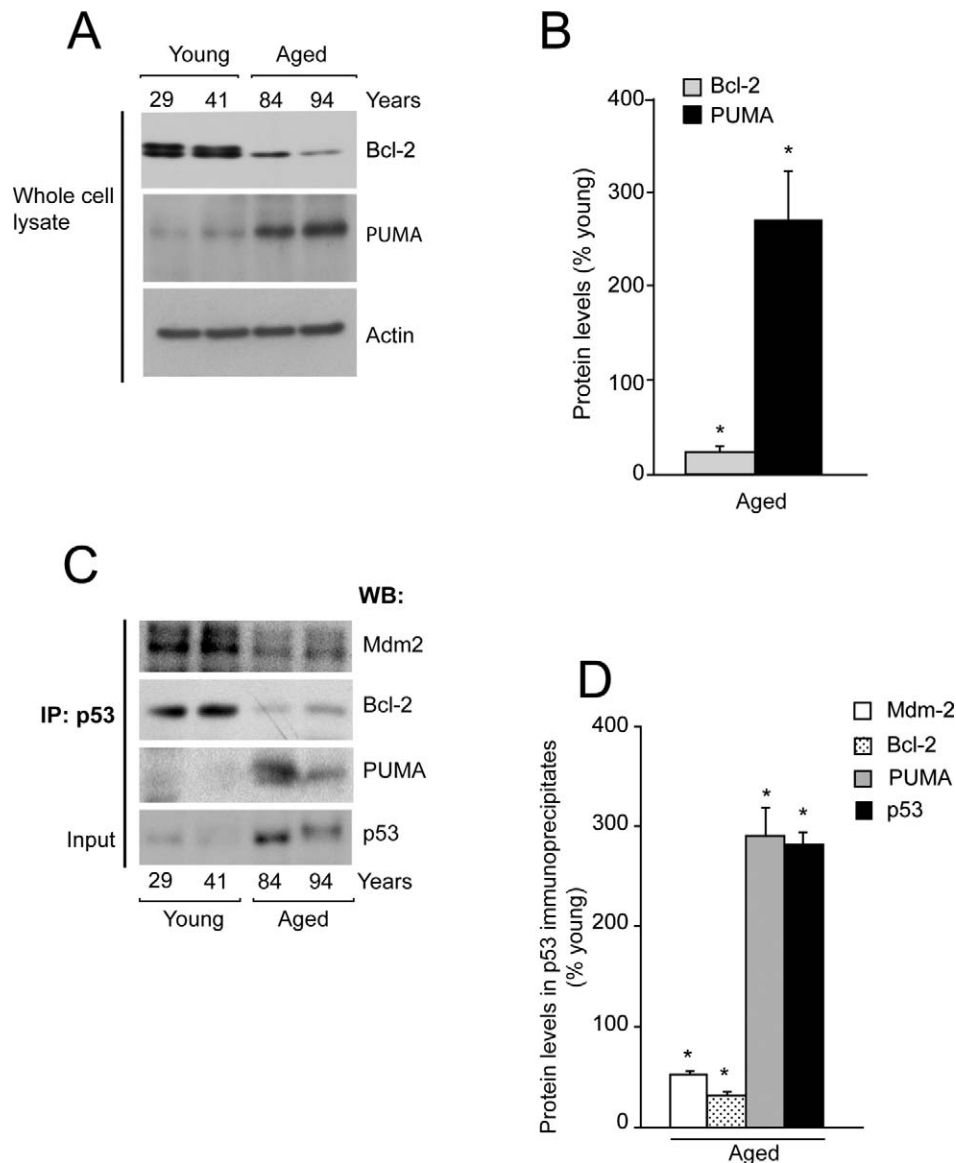


**FIGURE 3.** Age-dependent disruption of p53-Mdm2 binding. RPE cells isolated from young and aged donors were grown to confluence. (A) Cell lysates were analyzed by Western blot for the expression of Bcl-2 and PUMA. Actin was used as a loading control. (B) Densitometric analysis of results shown in (A). Values from young RPE cells were set at 100%. \*, significantly different compared with young RPE cells ( $P < 0.05$ ). (C) Cell lysates were immunoprecipitated using p53 antibody and immunoprecipitates were analyzed by Western blot using Mdm2, Bcl-2, and PUMA-specific antibodies. Blots were stripped and probed using p53 antibody (total input). (D) Densitometric analysis of results shown in (C). Values from young RPE cells were set at 100%. \*, significantly different compared with young RPE cells ( $P < 0.05$ ).

treatment with Nutlin-3. Consistent with our previous observations,<sup>15</sup> Nutlin-3 increased expression, and phosphorylation, of p53 in young RPE cells. In addition, data presented in Figures 5C and 5D show that Nutlin-3 increased acetylation of p53, which in turn induced caspase-9 and -3 activation and RPE apoptosis. Pretreatment of cells with Resveratrol significantly prevented Nutlin-3-induced increases in p53 acetylation and phosphorylation. As a result, RPE cells were significantly protected from Nutlin-3-induced apoptosis (Figs. 5C, 5D). Conversely, pretreatment of RPE cells with Sirtinol increased basal and Nutlin-3-induced p53 acetylation (Figs. 5C, 5D). Increased levels of p53 phosphorylation were also observed in cells treated with Sirtinol and Nutlin-3, respectively. Sirtinol alone increased caspase-9 and -3 activation. However, treatment of cells with Sirtinol plus Nutlin-3 potentiated apoptosis,

as evident by the increased levels of active caspase-9 and -3 (Figs. 5C, 5D), suggesting that sirtuins modulate p53 activation and, consequently, apoptosis in RPE cells.

### Sirtinol and Nutlin-3 Inhibit RPE Proliferation

Since Sirtinol and Nutlin-3 increased p53 activation and apoptosis in RPE cells, we tested whether these drugs could affect RPE proliferation. We reported earlier that transient treatment of RPE with a higher dose of Nutlin-3 (60  $\mu$ M) for 2 to 3 hours led to an overshoot in p53 levels and consequently triggered apoptosis.<sup>15</sup> To determine whether sustained p53 signaling using a low dose of Nutlin-3 would have similar consequences, we treated young RPE cells with 5  $\mu$ M Nutlin-3 for an extended time period. Treatment of proliferating cells with 25  $\mu$ M Sirtinol or 5  $\mu$ M Nutlin-3 for 48 hours in the

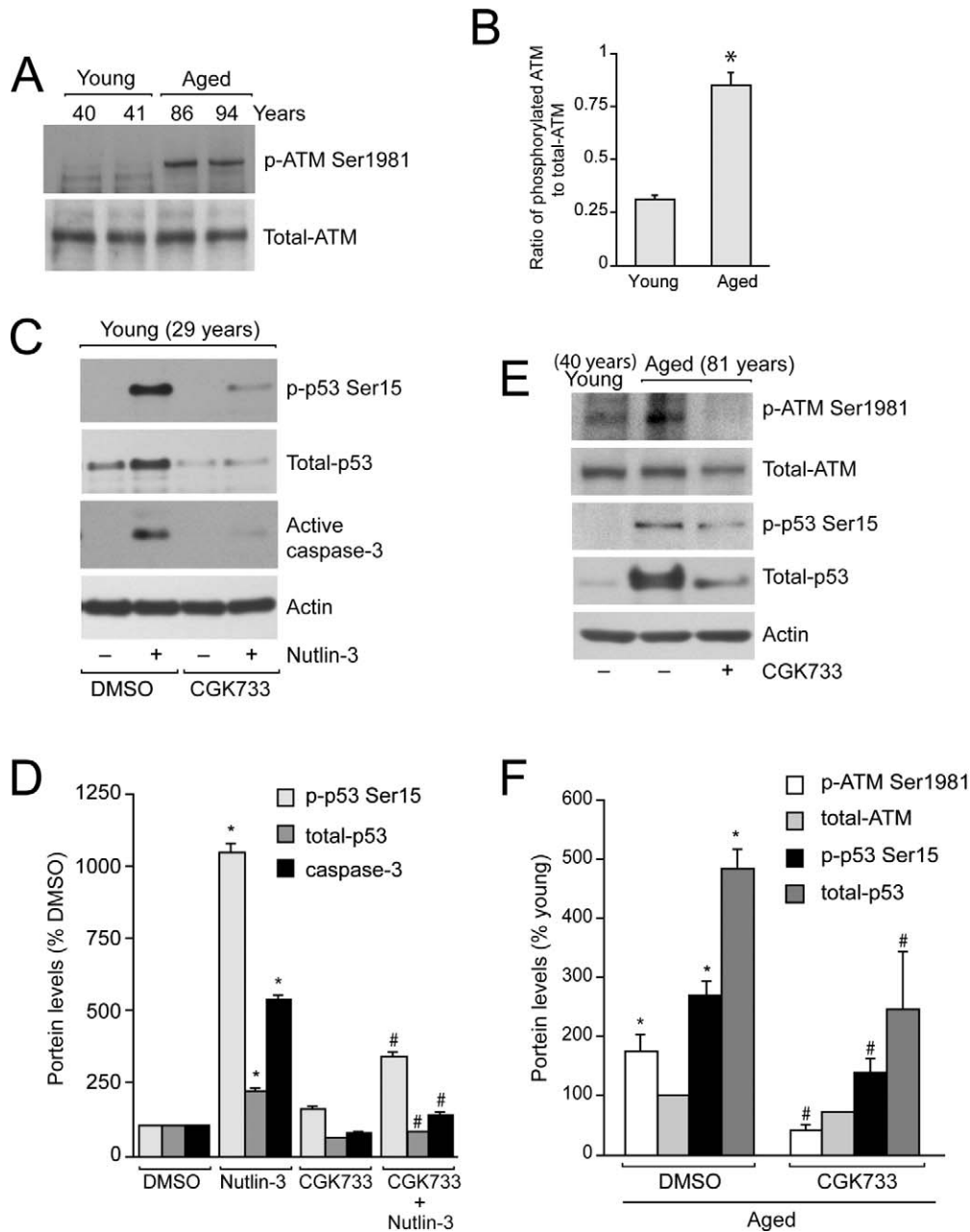


**FIGURE 4.** ATM/ATR kinase activates p53 in RPE cells. (A) Confluent RPE monolayers obtained from young and aged human donors were analyzed by Western blot for the levels of phospho-ATM Ser1981 and total-ATM using specific antibodies. (B) Densitometric analysis of phosphorylated and total ATM levels. \*, significantly different compared with young RPE cells ( $P < 0.05$ ). (C) RPE cells from young donors were pretreated with ATM/ATR kinase inhibitor (CGK733, 10  $\mu$ M) for 1 hour followed by treatment with 60  $\mu$ M Nutlin-3 for 2 hours. Equal volume of DMSO was used as control. Samples were analyzed for phospho-p53 Ser15, total-p53, and active caspase-3. (D) Densitometric analysis of results shown in (C). \*, significantly different compared with young RPE cells treated with DMSO; #, significantly different from young RPE cells treated with Nutlin-3 ( $P < 0.05$ ). (E) Confluent monolayers of aged RPE cells were treated overnight with CGK733 (10  $\mu$ M). Levels of phospho-ATM Ser1981, total-ATM, phospho-p53 Ser15, and total-p53 were compared with young RPE cells using specific antibodies. Actin was used as an internal loading control. (F) Densitometric analysis of results shown in (E). Values from young RPE cells were set at 100%. \*, significantly different compared with young RPE cells; #, significantly different compared with aged RPE cells treated with DMSO ( $P < 0.05$ ).

presence of serum containing medium significantly decreased cell numbers compared with DMSO-treated control cells, indicating decreased rates of proliferation (Fig. 6A). However, treatment of proliferating cells with the same concentrations of Sirtinol and Nutlin-3 had no effect on caspase-3 activation (Fig. 6B). Sirtinol increased p53 phosphorylation, acetylation, and protein levels but had no effect on Mdm2 and Mdm4

expression (Fig. 6B). Similar to the effect of Sirtinol, Nutlin-3 significantly increased p53 protein with a concomitant upregulation of its phosphorylation and acetylation (Fig. 6B). Interestingly, levels of p53 phosphorylation were significantly higher compared with p53 acetylation in response to Sirtinol and Nutlin-3 (Fig. 6B). Both Mdm2 and Mdm4 expression significantly increased in response to



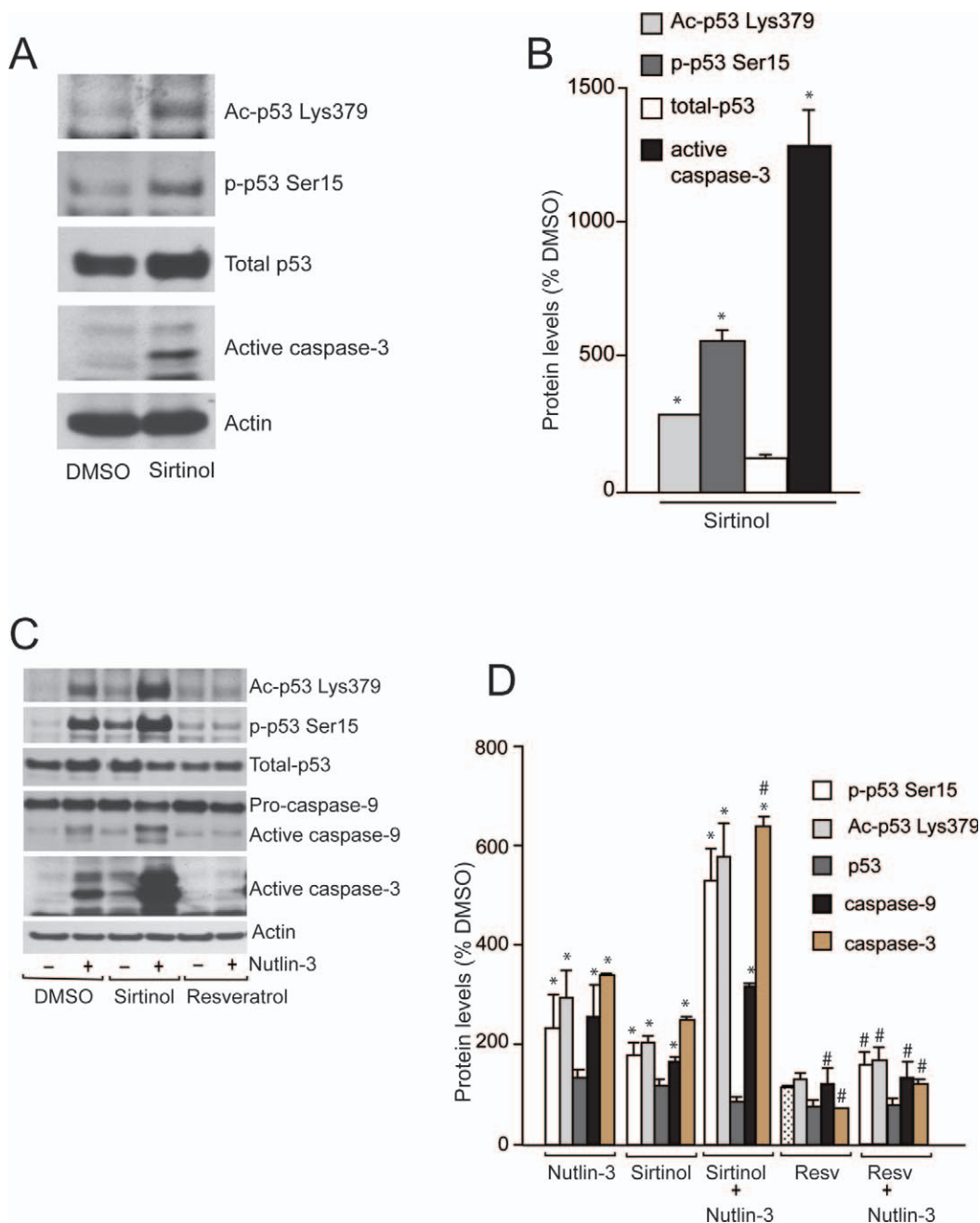


**FIGURE 5.** SIRT1/2 and RPE apoptosis. **(A)** Confluent serum starved RPE cells from young donor eyes (29 years of age) were treated with 50  $\mu$ M Sirtinol for 48 hours and cell lysates were prepared. Western blot for changes in protein levels for phospho Ser15, acetyl-Lys379, total p53, active caspase-3, and actin are shown. **(B)** Densitometric analysis of results shown in **(A)**. Values from DMSO-treated cells were set at 100%. \*, significantly different compared with cells treated with DMSO ( $P < 0.05$ ). **(C)** Confluent serum-starved RPE cells from young donor eyes (40 years of age) were pretreated with or without 50  $\mu$ M Sirtinol and 25  $\mu$ M Resveratrol for 18 to 20 hours followed by treatment with 60  $\mu$ M Nutlin-3 for 2 hours. Cell lysates were analyzed for the levels of phospho-53 Ser15, acetyl-p53 Lys379, total p53, active caspase-9, and active caspase-3 using specific antibodies. Actin was used as a loading control. **(D)** Densitometric analysis of results shown in **(C)**. Values from DMSO-treated cells were set at 100%. \*, significantly different compared with untreated cells; #, significantly different compared with Nutlin-3-treated cells ( $P < 0.05$ ). Resv, Resveratrol.

Nutlin-3 treatment, which is consistent with our previous observations.<sup>15</sup> Unphosphorylated retinoblastoma tumor suppressor protein (Rb) prevents cell cycle progression by binding with E2F family transcription factors, whereas phosphorylation of Rb by Cdk/cyclin complexes results in the release of bound E2F to stimulate transcription of genes involved in DNA synthesis and S-phase progression.<sup>52</sup> As

expected, levels of phosphorylated Rb (p-Rb) were found to be markedly lower in Sirtinol and Nutlin-3-treated cells. However, total Rb protein expression did not change in response to Sirtinol and Nutlin-3. Our results indicate that pharmacologically sustained p53 signaling (using lower concentrations of both Sirtinol and Nutlin-3) inhibits RPE proliferation without causing apoptosis.

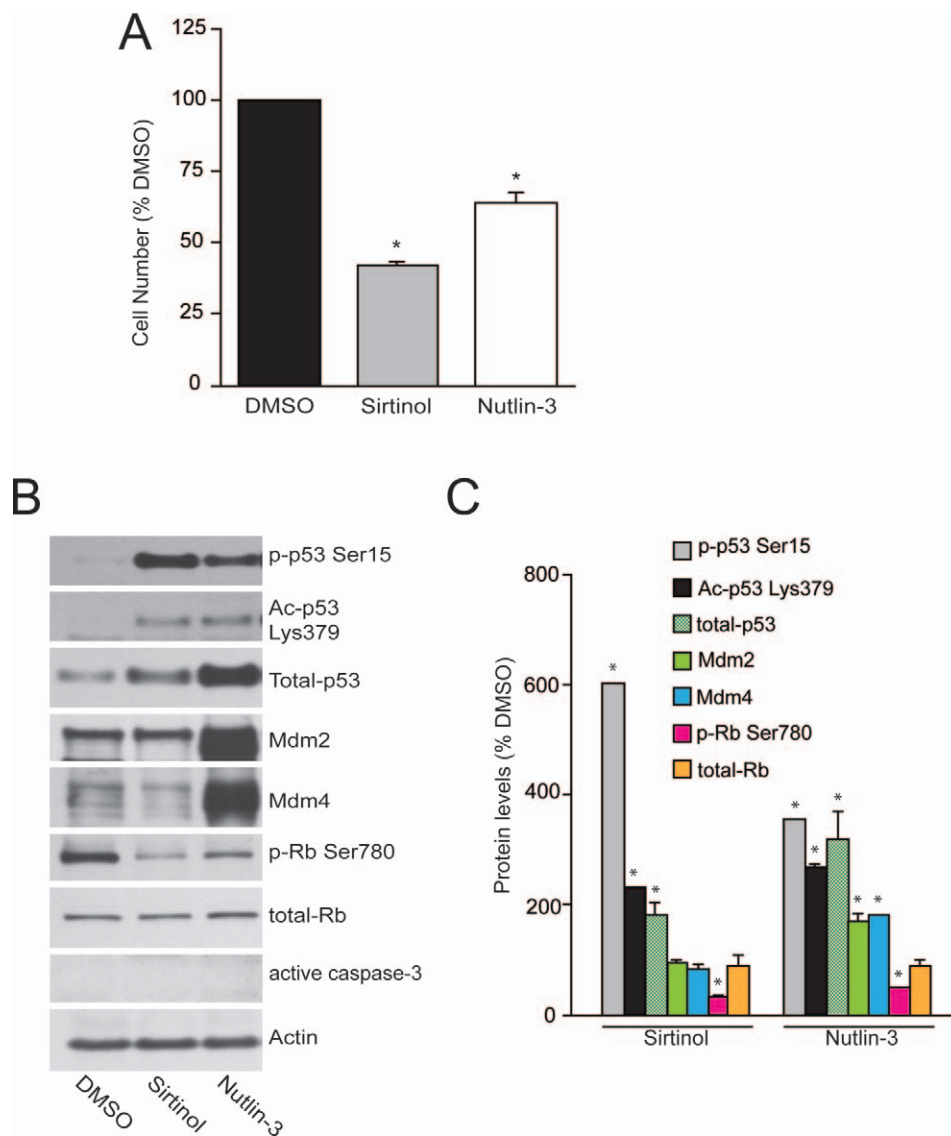


**FIGURE 6.** Sirtinol and Nutlin-3 inhibit proliferation of RPE cells. RPE cells from young donor eyes (40 years of age) were trypsinized and equal numbers of cells were seeded in serum-containing medium. Eighteen hours later the attached cells were treated with 25  $\mu$ M Sirtinol and 5  $\mu$ M Nutlin-3 and grown for 48 hours in serum-containing medium. (A) The cells were trypsinized and counted. \*, significantly different compared with DMSO-treated cells ( $P < 0.05$ ). (B) Cell lysates were analyzed by Western blot for the levels of phospho-p53 Ser15, acetyl-p53 Lys379, total p53, Mdm2, Mdm4, phospho-Rb Ser780, total-Rb, and active caspase-3. Actin was used an internal loading control. (C) Densitometric analysis of results shown in (B). Values from DMSO treated cells were set at 100%. \*, significantly different compared with cells grown in the presence of DMSO ( $P < 0.05$ ).

### Proteasome Inhibition Induces p53-Dependent Apoptosis in RPE Cultures

The ubiquitin-proteasome degradation pathway targets p53 for degradation and is a key regulator of cell survival.<sup>53</sup> Since data presented in Figure 3 show that expression of p53 increases as a function of age in RPE cells, we investigated whether inhibition of the ubiquitin-proteasomal pathway in young RPE cells could reproduce components of the p53-signaling axis seen in aged RPE cells. Overnight treatment of young RPE monolayers with 10  $\mu$ M MG132 increased acetylation and expression of p53 (Figs. 7A, 7B). Furthermore, Mdm2 and Mdm4 expression increased in response to MG132 (Figs. 7A, 7B). These results suggest that MG132 increased the stabilization and accumulation of p53, which in turn triggered caspase-

3 activation (Figs. 7A, 7B), DNA fragmentation (Fig. 7C), and sensitized young RPE cells to apoptosis, suggesting that the ubiquitin-proteasomal pathway is a pivotal regulator of p53 homeostasis and function.

### Knockdown of p53 Inhibits RPE Apoptosis

Since overall observations thus far indicate a role for p53 in age-associated RPE apoptosis, we examined the effect of inhibiting p53 expression by siRNA. Specificity of p53 knockdown was confirmed by a significant decrease in total p53 protein in young RPE cells transfected with p53-siRNA but not in cells transfected with control siRNA (Figs. 8A, 8B). Consistent with our previous observations in Figure 5C, Nutlin-3 upregulated p53, which in turn caused caspase-3 activation

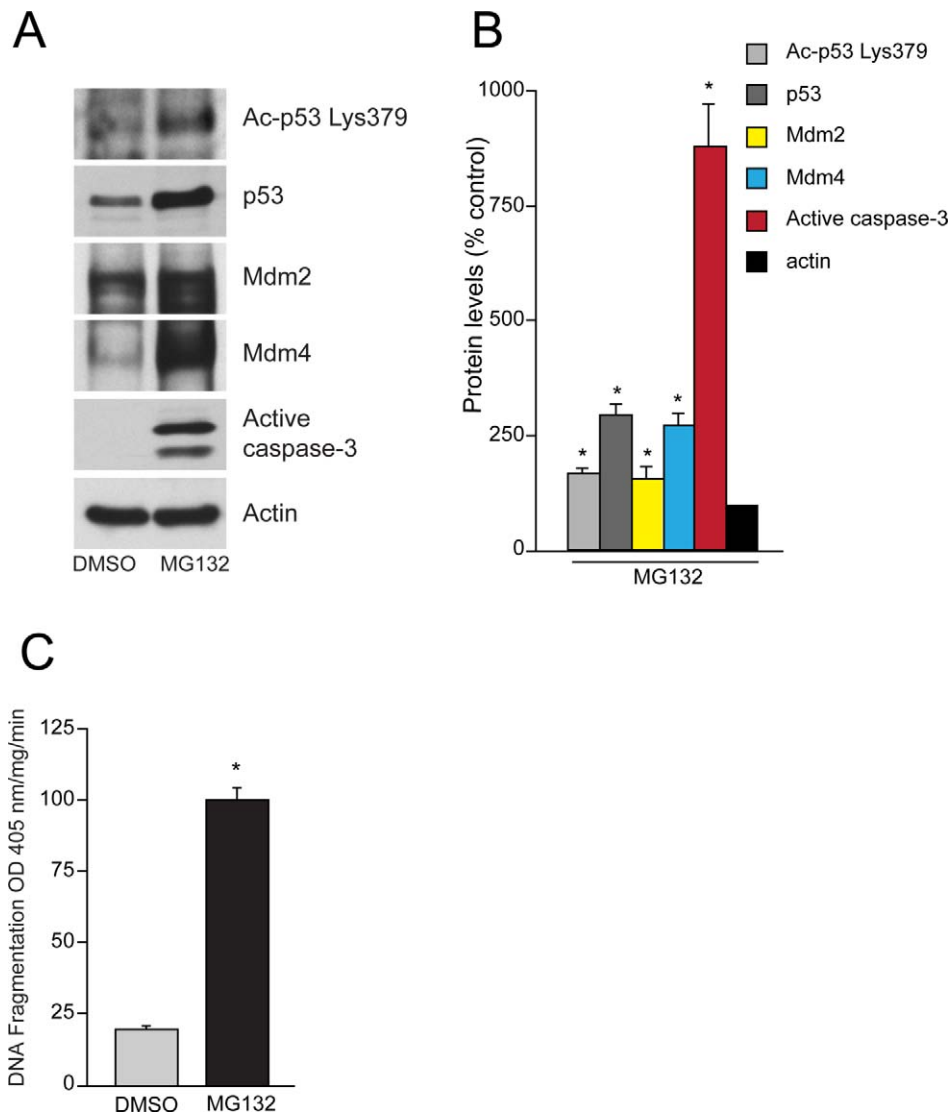


**FIGURE 7.** Inhibition of ubiquitination by MG132 sensitizes young RPE cells to p53-dependent apoptosis. **(A)** RPE cells from young donor eyes (41 years of age) were treated with 10  $\mu$ M MG132 for 18 hours, and lysates were subjected to Western blot analysis for the levels of acetylated p53 Lys379, total p53, Mdm2, Mdm4, and active caspase-3 using specific antibodies. Actin was used as a loading control. **(B)** Densitometric analysis of results shown in **(A)**. Values from DMSO-treated young cells were set at 100%. \*, significantly different compared with cells treated with DMSO ( $P < 0.05$ ). **(C)** Confluent monolayers of RPE cells from young donor eyes (40 years of age) were treated with DMSO or 10  $\mu$ M MG132 overnight. DNA fragmentation was measured by ELISA (mean  $\pm$  SEM,  $n = 3$ ). \*, significantly different compared with cells treated with DMSO ( $P < 0.05$ ).

and apoptosis (Figs. 8A, 8B). Conversely, Nutlin-3 failed to upregulate p53 in RPE cells transfected with p53 siRNA and, consequently, inhibited caspase-3 activation and apoptosis (Figs. 8A, 8B). In addition, knockdown of p53 in aged RPE (Figs. 8C, 8D) inhibited caspase-3 and, consequently, decreased age-related apoptosis (Figs. 8C, 8D). These results suggest that apoptosis of aging RPE cells is p53-dependent.

### Drugs Modulating p53/Mdm2 Signaling and Human RPE Apoptosis

A comprehensive summary of different drugs modulating the p53/Mdm2-signaling axis in human RPE and their modes of action on phosphorylation, acetylation, and expression of p53 are described in Table 2. Mdm2 antagonist, Nutlin-3, was used to inhibit the interaction of p53 with Mdm2, which triggered p53 activation and RPE apoptosis. The proteasome inhibitor, MG132, prevented degradation of proteins, which in turn

accumulated p53 and triggered RPE apoptosis. Specific inhibition of Sirtuins (both SIRT1/2) by Sirtinol activated p53 and caused RPE death. Conversely, activation of Sirtuins by Resveratrol decreased activation of p53 and prevented RPE death. Inhibition of ATM/ATR kinases by CGK733 blocked p53 phosphorylation, which in turn destabilized p53 and increased Mdm2-dependent degradation. As a result, p53 expression decreased and RPE cells were protected from apoptosis.

### DISCUSSION

The key finding of our studies is that RPE from aged donors exhibits fundamental differences in intrinsic p53 pathways compared with RPE from young donors. The overall effect of these differences is that aged RPE has higher rates of p53-dependent apoptosis. The increase in apoptosis during physiologic aging was documented by the presence of caspase-3 activation, DNA fragmentation, and TUNEL-positive



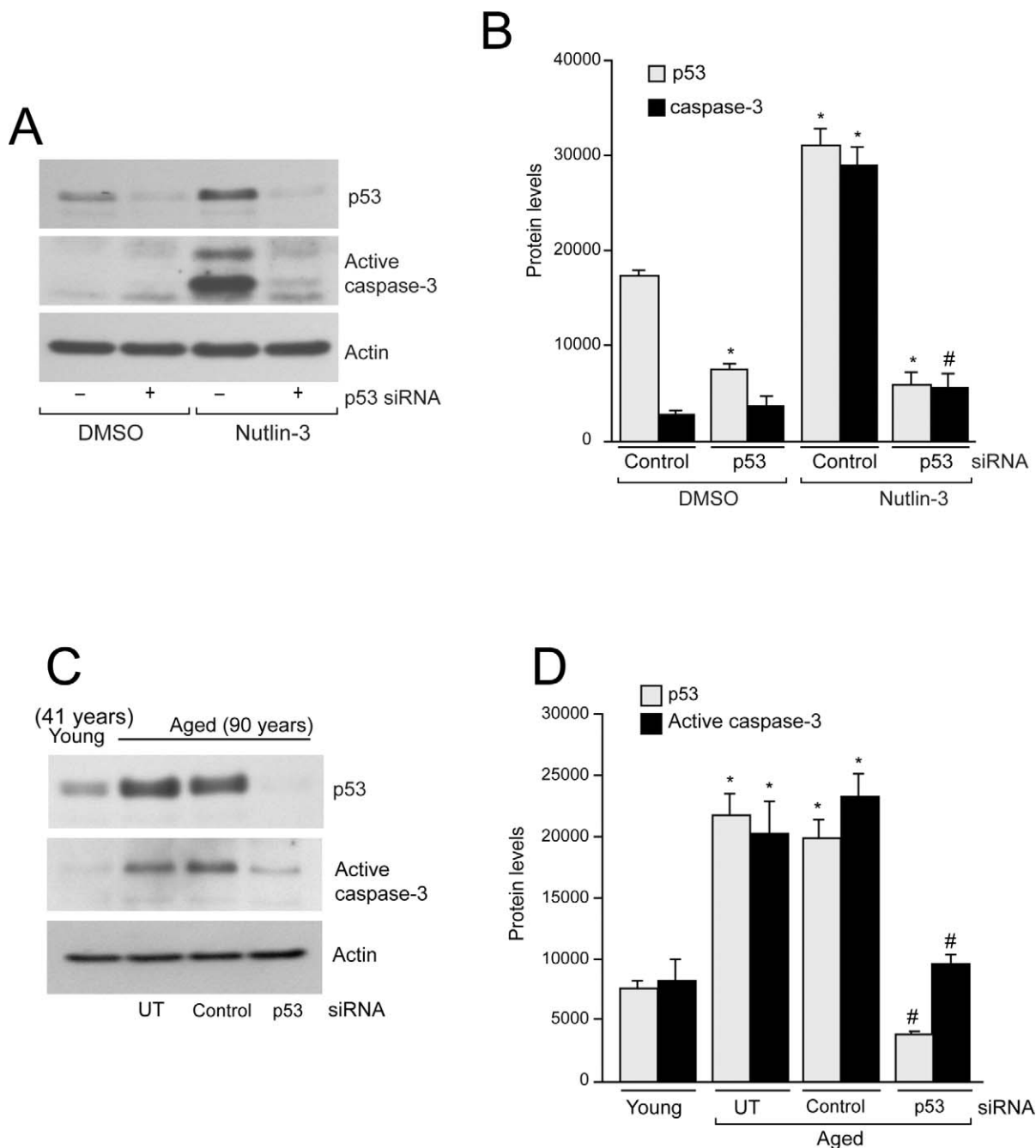


**FIGURE 8.** Knockdown of p53 by gene-specific siRNA inhibits RPE apoptosis. RPE cells obtained from young donor eyes (29 years of age) were transfected with control or p53-specific siRNA as described in experimental procedures and treated with 60  $\mu$ M Nutlin-3 for 2 hours. (A) Cell lysates were analyzed by Western blots for the levels of total p53, and active caspase-3 using specific antibodies. Membranes were stripped and probed for actin as an internal loading control. (B) Densitometric analysis of results shown in (A). \*, significantly different compared with untreated cells; #, significantly different compared with Nutlin-3 treated cells ( $P < 0.05$ ). (C) RPE cells obtained from aged donors were either left untreated (UT) or transfected with control or p53-specific siRNA. Total-p53 and active caspase-3 levels were compared with RPE cells from young donors using specific antibodies. (D) Densitometric analysis of results shown in (C). \*, significantly different compared with young RPE; #, significantly different compared with aged RPE cells transfected with control siRNA ( $P < 0.05$ ).

RPE cells (Fig. 1), which are hallmarks of apoptosis. These findings support earlier reports of age-dependent apoptosis in human RPE<sup>54</sup> and loss of RPE in patients with AMD.<sup>55</sup>

Based on a comparison of gene expression, posttranslational protein modification, and pharmacologic interactions in cultured RPE cells from old versus young donors, the major age-related alteration in the p53 pathway was found to be the stabilization of free p53 (unbound to Mdm2) associated with

increased rates of phosphorylation and acetylation of the p53 protein (Figs. 2B, 2C). Because of the increase in free p53 (Fig. 2A) and relative lack of Mdm2 sequestration (Figs. 3C, 3D), subsequent steps in the apoptotic pathway, including p53-dependent upregulation of de novo synthesis of BH3-only proapoptotic PUMA (Figs. 3A, 3B), then proceed at an accelerated pace in aged RPE. Importantly, this finding was confirmed in intact retinal tissue from normally aged Fisher

TABLE 2. Drugs Used along with Their Effect on Phosphorylation, Acetylation, p53 Expression, and RPE Apoptosis

Drugs	Mode of Action	Effect on p53 Phosphorylation	Effect on p53 Acetylation	Effect on p53 Expression	Effect on RPE Apoptosis
Nutlin-3	Inhibits Mdm2-p53 interaction	Increased	Increased	Increased	Increased
CGK733	Selective ATM/ATR kinase inhibitor	Decreased	Not known	Decreased	Decreased
Sirtinol	Specific inhibitor of the sirtuin class of deacetylase activity	Increased	Increased	No change	Increased
Resveratrol	Reported to activate NAD <sup>+</sup> -dependent histone deacetylase SIRT1	Decreased	Decreased	No change	Decreased
MG132	Inhibits the degradation of ubiquitin-conjugated proteins	Not known	Increased	Increased	Increased

344×Brown Norway F1 hybrid rats, which show increased p53 protein as well as p53 mRNA (32 months of age) compared with younger controls (8 months of age) (Steinle JJ, personal written communication, 2011), suggesting that posttranslational modification of p53 during aging leads to increased stability. Moreover, p53 has been linked to retinal apoptosis in specific cell types.<sup>56</sup> Our p53 siRNA studies further support the participation of p53 signaling in apoptosis of RPE cells. Treatment of aged RPE with p53 siRNA caused a knockdown of p53 expression, leading to a direct decrease in caspase-3 activation and apoptosis (Figs. 8C, 8D). Additionally, p53 siRNA prevented the induction of p53 expression in young RPE, normally observed after Nutlin-3 inhibition of Mdm2 (Figs. 8A, 8B). Concomitantly, caspase-3 activity and apoptosis were attenuated. Based on these findings, we propose that accumulation of activated p53 during aging may be a decisive factor in the onset of apoptosis in the retina, specifically in RPE, and may represent a contributory factor in age-related retinal degeneration.

Consistent with the notion of a link between activated p53 and degenerative pathologies of aging in general,<sup>57</sup> dysregulated expression of p53 in mice has been shown to result in a variety of age-related phenotypes.<sup>34,58</sup> However, the full complement of p53 actions may be complex, show cell type specificity, and have some effects not directly related to PUMA and apoptotic pathways. For example, p53 can lead to premature senescence in fibroblasts through activation of aberrant genes.<sup>19</sup> In addition, p53 is also known in some instances to suppress senescence due to its ability to negatively regulate mTOR and Akt signaling.<sup>59</sup> Therefore, p53 has been implicated in both promoting and inhibiting longevity in animal models. To avoid the complexity that might result from mixed cell populations in whole tissue, we chose to use cultured RPE cells for most of our studies, because this allowed us to identify the age-related changes in the p53 pathway that are specifically related to this cell type and that are linked to both cell death and other age-related changes as discussed in the following text.

Through analysis of many of the independent components of the p53 pathway, we first determined which individual elements showed age-dependent changes and which did not. The most significant change noted was an increase in posttranslational modification of p53 by both phosphorylation and acetylation (Figs. 2B, 2C), with a concomitant decrease in sequestration by Mdm2 (Figs. 3C, 3D). Our previous studies in RPE have shown that blocking p53-Mdm2 binding (using Nutlin-3) effectively elevated p53 function and sensitized young RPE cells to apoptosis via increased expression of BH3-only proapoptotic proteins PUMA and Noxa.<sup>15</sup> Given that posttranslational modifications of p53 would thus be expected to induce apoptosis, we next considered what other well-established changes during aging might trigger these modifi-

cations. Age-related oxidative DNA damage has been reported in the retina,<sup>60</sup> suggesting that prolonged exposure to oxidative stress throughout a person's lifetime may cause cumulative DNA damage, which leads to the activation of intrinsic repair enzymes including H2AX and ATM/ATR kinases. ATM is rapidly autophosphorylated in response to ionizing radiation or chemotherapeutic drugs,<sup>61</sup> resulting in the phosphorylation of several targets, such as Chk2 and, importantly, p53. ATR phosphorylates p53 on Ser15 and Ser37 in response to DNA replication inhibitors (hydroxyurea and ionizing radiation), confirming that p53 is a target for ATM/ATR.<sup>62</sup> Simultaneously, phosphorylated H2AX accumulates at the sites of double-stranded DNA breaks and recruits other components of the DNA repair machinery.<sup>63</sup> In accordance with this proposed mechanism, we observed increased phosphorylation of H2AX (Figs. 2B, 2C) and ATM kinase (Figs. 4A, 4B) in RPE from aged donors. Pretreatment of young RPE cells with the ATM/ATR inhibitor, CGK733, blocked Nutlin-3-induced phosphorylation of p53 at Ser15 and protected cells from apoptosis (Figs. 4C, 4D). Furthermore, CGK733 decreased phosphorylation of p53 in aged RPE cells (Figs. 4E, 4F), strongly suggesting that ATM/ATR are the upstream kinases responsible for the age-related phosphorylation and activation of p53.

Although the rate of acetylation of p53 depends on binding to p300/CREB-binding protein, the rate of p53 deacetylation by SIRT1 also appears to play a significant regulatory role. SIRT1 is expressed throughout the retina, including retinal ganglion cells, photoreceptors, and RPE cells.<sup>64</sup> Deletion of the upstream activator of SIRT1 causes retinal cell death concomitant with hyperacetylation of p53.<sup>65</sup> Our findings using SIRT1 inhibitor are consistent with these reports. Inhibition of SIRT1/2 in young RPE by Sirtinol increased acetylation of p53 and induced caspase-3-dependent RPE apoptosis (Figs. 5A, 5B). Because acetylation of p53 alters its structure,<sup>66</sup> it is possible that once p53 is acetylated, its resulting conformational change leads to increased association with proapoptotic Bcl-2 family proteins including Bax and PUMA. Consequently, p53-Bax or p53-PUMA complexes translocate to the mitochondria, leading to the release of cytochrome C,<sup>67,68</sup> followed by activation of caspases-9, -3, and apoptosis. Therefore, it appears that SIRT's deacetylate the tumor suppressor protein p53 and attenuate cell death.

Sirtinol was found to inhibit both SIRT1 and SIRT2 and induce p53 acetylation.<sup>69</sup> Acetylation of p53 in response to sustained stress preferentially activates cell-cycle arrest.<sup>70</sup> Treating young RPE cells with low concentrations of Sirtinol (25  $\mu$ M) in the presence of serum-containing medium during proliferation significantly decreased cell numbers (Fig. 6A), without inducing apoptosis (Fig. 6B). This was accompanied by phosphorylation, acetylation, and expression of p53, indicating that SIRT1/2-dependent modification of p53 dictates

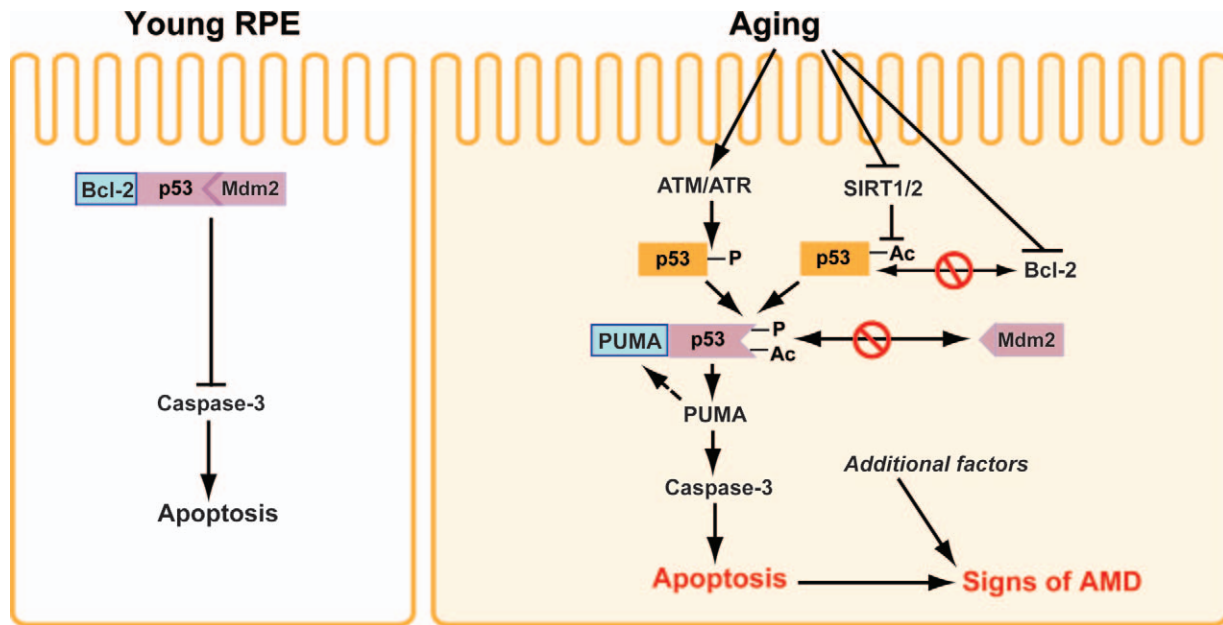


**FIGURE 9.** Schematic representation of age-dependent p53–Mdm2 signaling in human RPE. In RPE cells from young donors, the p53 protein is kept at low activity levels via its association with Mdm2 (E3 ubiquitin ligase). As a result, p53 cannot upregulate synthesis of proapoptotic PUMA. Furthermore, antiapoptotic Bcl-2 binds and sequesters p53 and consequently cells are resistant to apoptosis. In RPE cells from aged donors, decreased expression of antiapoptotic Bcl-2 and its reduced association with age-modified p53 increase susceptibility to apoptosis. Aging of RPE results in the phosphorylation (-P) of p53 by ATM/ATR kinases. Simultaneously, age-related inhibition of histone deacetylase (SIRT1/2) favors acetylation (-Ac) of p53. Both phosphorylation and acetylation of p53 inhibit its binding with Mdm2 and lead to its stabilization and activation. Overactive p53 in RPE from aged human donors allows nascent synthesis of PUMA. In addition, PUMA complexes with p53 and, consequently, triggers caspase-3–dependent apoptosis. Increased RPE apoptosis coupled with environmental and genetic factors set the stage for the pathogenesis of AMD.

RPE proliferation (Fig. 6). Others have found that exposure to 50  $\mu$ M Sirtinol for 48 hours inhibited proliferation of breast carcinoma cell lines.<sup>69</sup> In addition; low concentrations of Nutlin-3 (5  $\mu$ M) increased phosphorylation, acetylation, and expression of p53 (Figs. 6B, 6C) and, consequently, inhibited RPE proliferation (Fig. 6A).

We reported earlier that the Mdm2 antagonist, Nutlin-3, increases phosphorylation of p53 at Ser15<sup>15</sup>; however, our current study shows that Nutlin-3 treatment increases acetylation of p53 as well. It is known that Mdm2 inhibits p300-mediated p53 acetylation by forming a ternary complex with these two proteins.<sup>71</sup> Based on our results, it is intriguing to postulate that either phosphorylation of p53 acts as a rheostat and increases its affinity to p300/CREB-binding protein, or inhibition of Mdm2 prevents the formation of Mdm2-p53-p300 complex and ultimately favors the acetylation of p53. Taken together these results suggest that SIRT1/2 acts to keep p53 deacetylated and more accessible to Mdm2 sequestration in young RPE.

Resveratrol is known to have antiangiogenic, neuroprotective, and antioxidant properties and regulates lifespan by its ability to activate histone deacetylase SIRT1.<sup>72</sup> Our data show that Resveratrol blocked Nutlin-3-mediated phosphorylation and acetylation of p53 and eventually inhibited caspase-3 activation (Figs. 5C, 5D). Our data suggest for the first time that Resveratrol is a potential drug candidate that could be used to protect RPE cells from apoptosis, and that the extent of posttranslational modification and stabilization of p53 appears to be critical in determining whether RPE undergo apoptosis.

Cellular p53 protein is tightly regulated by ubiquitin-dependent degradation of p53. Inhibition of proteasome and ubiquitination with MG132 reversed the degradation of p53

and dramatically increased the amount of p53 in young RPE cells (Fig. 7). Furthermore, MG132 increased p53 acetylation (i.e., activation) and increased the accumulation of Mdm2 and Mdm4, which caused increased stabilization of p53 and subsequent caspase-3–dependent apoptosis. In a recent report Uchiki et al.<sup>73</sup> suggested the involvement of the ubiquitin-proteasome system in the degradation of advanced glycation end products. Another study showed that E3 mono-ubiquitin ligase Bmi1 is downregulated in the aging brain, leading to activation of p53 and subsequent upregulation of inflammatory and senescence markers.<sup>36</sup> Therefore, it is clear that ubiquitin ligases represent a mechanism by which p53 activation and apoptosis are regulated in the aging RPE.

In addition to an increase in posttranslational modification of p53, we also noted an age-related decrease in expression of the antiapoptotic protein, Bcl-2. It is known that proapoptotic Bcl-2 family members Bax, Bak, Bid, PUMA, and cytosolic p53 are sequestered by the antiapoptotic Bcl-2 family proteins (e.g., Bcl-2, Bcl-xL, and Mcl-1). We observed high levels of Bcl-2 expression in young RPE cells (Figs. 3A, 3B), and immunoprecipitation of p53 effectively brought down Bcl-2 (Figs. 3C, 3D), suggesting that Bcl-2 sequesters p53 (rendering p53 inactive) and controls the integrity of the outer mitochondrial membrane. In aged cells, a coordinated effort between previously sequestered and nascent PUMA results in the inhibition of p53 sequestration by Bcl-2, leading to permeabilization of the outer-mitochondrial membrane, which finally culminates in apoptosis.

Increased rates of apoptosis also correlated with the discontinuity of the RPE monolayer, indicating that the integrity of the intercellular junctions was compromised during aging (Fig. 1D). It is reasonable to speculate that the



age-related alterations of tight and adherens junctions in RPE could be caused by caspase-3-dependent proteolytic degradation of ZO-1 and beta-catenin. ZO-1 is cleaved by active caspase-3 in epithelial cells,<sup>74</sup> and apoptotic cell death is associated with proteolysis of beta-catenin.<sup>75</sup> Others have shown that inhibition of caspase-3 activity blocked beta-catenin degradation after focal ischemia.<sup>76</sup> However, it is unclear whether aging alters the RPE phenotype by remodeling the distributions of cell adhesion and junction proteins, or whether these alterations reflect preapoptotic changes. Further investigation is necessary to address how increased apoptosis in aging RPE might contribute to the impairment of tight and adherens junctions.

In conclusion, our current model suggests that p53 is largely inactivated in RPE from young human donors due to its association with Mdm2 and Bcl-2 (Fig. 9). Normal aging involves stress from reactive oxygen and nitrogen intermediates, leading to DNA damage. As a result, ATM/ATR kinases are activated, which in turn phosphorylate p53. Simultaneously, aging downregulates histone deacetylase SIRT1/2, which favors the acetylation of p53. Age-dependent phosphorylation and acetylation of p53 lead to decreased Mdm2 binding, which frees and stabilizes p53 to upregulate transcription of proapoptotic inducer PUMA and consequently to trigger RPE apoptosis (Fig. 9). Furthermore, comparative analysis revealed that aging RPE cells display a downregulation of antiapoptotic Bcl-2 protein. In testing our model, we found that pharmacologic intervention of the p53/Mdm2-signaling axis induced young RPE cells to die, as do aged cells. Likewise, using p53-specific siRNA and Resveratrol, we were able to protect RPE cells from apoptosis, suggesting that p53 is a key regulator involved in the dysfunction of human RPE. Our findings add to our overall understanding of age-related changes in RPE and further suggest that drugs that block acetylation/phosphorylation of p53 represent promising targets for future therapeutics.

### Acknowledgments

The authors thank the National Disease Research Interchange (NDRI) for providing postmortem human donor eyes of various ages, Shyamali Basuroy for assistance with confocal microscopy, and Jena J. Steinle at the Hamilton Eye Institute for critically reading the manuscript.

### References

- Friedman DS, O'Colmain BJ, Muñoz B, et al; Eye Diseases Prevalence Research Group. Prevalence of age-related macular degeneration in the United States. *Arch Ophthalmol*. 2004;122:564-572.
- Green WR. Histopathology of age-related macular degeneration. *Mol Vis*. 1999;3:5-27.
- Bonilha VL. Age and disease-related structural changes in the retinal pigment epithelium. *Clin Ophthalmol*. 2008;2:413-424.
- Nowak JZ. Age-related macular degeneration (AMD): pathogenesis and therapy. *Pharmacol Rep*. 2006;58:353-363.
- Marmor MF, Wolfensberger TJ. *The Retinal Pigment Epithelium: Function and Disease*. New York: Oxford University Press; 1998.
- Peng S, Rao VS, Adelman RA, Rizzolo LJ. Claudin-19 and the barrier properties of the human retinal pigment epithelium. *Invest Ophthalmol Vis Sci*. 2011;52:1392-1403.
- Bailey TA, Kanuga N, Romero IA, Greenwood J, Luthert PJ. Oxidative stress affects the junctional integrity of retinal pigment epithelial cells. *Invest Ophthalmol Vis Sci*. 2004;45:675-684.
- Zarbin MA. Current concepts in the pathogenesis of age-related macular degeneration. *Arch Ophthalmol*. 2004;122:598-614.
- Hamdi HK, Kenney C. Age-related macular degeneration: a new viewpoint. *Front Biosci*. 2001;8:e305-e314.
- Anderson DH, Radeke MJ, Gallo NB, et al. The pivotal role of the complement system in aging and age-related macular degeneration: hypothesis re-visited. *Prog Retin Eye Res*. 2010;29:95-112.
- Ding X, Patel M, Chan CC. Molecular pathology of age-related macular degeneration. *Prog Retin Eye Res*. 2009;28:1-18.
- Ambati J, Anad A, Fernandez S, et al. An animal model of age-related macular degeneration in senescent Ccl-2 or Ccr-2 deficient mice. *Nat Med*. 2003;9:1390-1397.
- Friedman DS, O'Colmain BJ, Muñoz B, et al. Prevalence of age-related macular degeneration in the United States. *Arch Ophthalmol*. 2004;122:564-572.
- Chen H, Liu B, Lukas TJ, Neufeld AH. The aged retinal pigment epithelium/choroid: a potential substratum for the pathogenesis of age-related macular degeneration. *PLoS One*. 2008;3:e2339.
- Bhattacharya S, Ray RM, Chaum E, Johnson DA, Johnson LR. Inhibition of Mdm2 sensitizes human retinal pigment epithelial cells to apoptosis. *Invest Ophthalmol Vis Sci*. 2011;52:3368-3380.
- Yang P, Peairs JJ, Tano R, Zhang N, Tyrell J, Jaffe GJ. Caspase-8-mediated apoptosis in human RPE cells. *Invest Ophthalmol Vis Sci*. 2007;48:3341-3349.
- Zhang N, Peairs JJ, Yang P, et al. The importance of Bcl-xL in the survival of human RPE cells. *Invest Ophthalmol Vis Sci*. 2007;48:3846-3853.
- Antony R, Lukiw WJ, Bazan NG. Neuroprotectin D1 induces dephosphorylation of Bcl-xL in a PP2A-dependent manner during oxidative stress and promotes retinal pigment epithelial cell survival. *J Biol Chem*. 2010;285:18301-18308.
- Levine AJ, Hu W, Feng Z. The p53 pathway: what questions remain to be explored? *Cell Death Differ*. 2006;13:1027-1036.
- Chuikov S, Kurash JK, Wilson JR, et al. Regulation of p53 activity through lysine methylation. *Nature*. 2004;432:353-360.
- Wu X, Bayle JH, Olson D, Levine AJ. The p53-mdm2 autoregulatory feedback loop. *Genes Dev*. 1993;7:1126-1132.
- Wade M, Wang YV, Wahl GM. The p53 orchestra: Mdm2 and Mdmx set the tone. *Trends Cell Biol*. 2010;20:299-309.
- Shvarts A, Steegenga WT, Riteco N, et al. Mdmx: a novel p53-binding protein with some functional properties of Mdm2. *EMBO J*. 1996;15:5349-5357.
- Shangary S, Wang S. Small-molecule inhibitors of the Mdm2-p53 protein-protein interaction to reactivate p53 function: a novel approach for cancer therapy. *Annu Rev Pharmacol Toxicol*. 2009;49:223-241.
- Xu Y. Regulation of p53 responses by post-translational modifications. *Cell Death Differ*. 2003;10:400-403.
- Banin S, Moyal L, Shieh S-Y, et al. Enhanced phosphorylation of p53 by ATM in response to DNA damage. *Science*. 1998;281:1674-1677.
- Ito A, Lai CH, Zhao X, et al. P300/CBP-mediated p53 acetylation is commonly induced by p53-activating agents and inhibited by Mdm2. *EMBO J*. 2001;20:1331-1340.
- Solomon JM, Pasupuleti R, Xu L, et al. Inhibition of SIRT1 catalytic activity increases p53 acetylation but does not alter cell survival following DNA damage. *Mol Cell Biol*. 2006;26:28-38.
- Bordone L, Guarente L. Calorie restriction, SIRT1 and metabolism: understanding longevity. *Nat Rev Mol Cell Biol*. 2005;6:298-305.

30. Blander G, Guarente L. The Sir2 family of protein deacetylases. *Annu Rev Biochem.* 2004;73:417-435.
31. Zhu Q, Wani G, Yao J, et al. The ubiquitin-proteasome system regulates p53-mediated transcription at p21waf1 promoter. *Oncogene.* 2007;26:4199-4208.
32. Alves-Rodrigues A, Gregori L, Figueiredo-Pereira ME. Ubiquitin, cellular inclusions and their role in neurodegeneration. *Trends Neurosci.* 1998;21:516-520.
33. Low P. The role of ubiquitin-proteasome system in ageing. *Gen Comp Endocrinol.* 2011;172:39-43.
34. Tyner SD, Venkatachalam S, Choi J, et al. p53 mutant mice that display early ageing-associated phenotypes. *Nature.* 2002;415:45-53.
35. Osorio FG, Varela I, Lara E, et al. Nuclear envelope alterations generate an aging-like epigenetic pattern in mice deficient in Zmpste24 metalloprotease. *Aging Cell.* 2010;9:947-957.
36. Abdouh M, Chatoo W, El Hajjar J, David J, Ferreira J, Bernier G. Bmi1 is down-regulated in the aging brain and displays antioxidant and protective activities in neurons. *PLoS One.* 2012;7:e31870.
37. Chaum E. Comparative analysis of the uptake and expression of plasmid vectors in human ciliary and retinal pigment epithelial cells in vitro. *J Cell Biochem.* 2001;83:671-677.
38. Bhattacharya S, Ray RM, Johnson LR. Role of polyamines in p53-dependent apoptosis of intestinal epithelial cells. *Cell Signal.* 2009;21:509-522.
39. Bhattacharya S, Ray RM, Johnson LR. Basic helix-loop-helix protein E47-mediated p21Waf1/Cip1 gene expression regulates apoptosis of intestinal epithelial cells. *Biochem J.* 2007;407:243-254.
40. Bhattacharya S, Ray RM, Johnson LR. Polyamines are required for activation of c-Jun NH<sub>2</sub>-terminal kinase and apoptosis in response to TNF- $\alpha$  in IEC-6 cells. *Am J Physiol Gastrointest Liver Physiol.* 2003;285:G980-G991.
41. Basuroy S, Seth A, Elias B, Naren AP, Rao R. MAPK interacts with occludin and mediates EGF-induced prevention of tight junction disruption by hydrogen peroxide. *Biochem J.* 2006;393:69-77.
42. Pollack M, Leeuwenburgh C. Apoptosis and aging: role of the mitochondria. *J Gerontol.* 2001;56A:B475-B482.
43. Bell JE, Sharpless NE. Telomeres, p21 and the cancer-aging hypothesis. *Nat Genet.* 2007;39:11-12.
44. Ju Z, Choudhury AR, Rudolph KL. A dual role of p21 in stem cell aging. *Ann N Y Acad Sci.* 2007;1100:333-344.
45. Burma S, Chen BP, Murphy M, Kurimasa A, Chen DJ. ATM phosphorylates histone H2AX in response to DNA double-strand breaks. *J Biol Chem.* 2001;276:42462-42467.
46. Lu C, Zhu F, Cho YY, et al. Cell apoptosis: requirement of H2AX in DNA ladder formation, but not for the activation of caspase-3. *Mol Cell.* 2006;23:121-132.
47. Roth J, Dobbstein M, Freedman DA, Shenk T, Levine AJ. Nucleo-cytoplasmic shuttling of the hdm2 oncoprotein regulates the levels of the p53 protein via a pathway used by the immunodeficiency virus rev protein. *EMBO J.* 1998;17:554-564.
48. Chen F, Chang D, Goh M, Klivanov SA, Ljungman M. Role of p53 in cell cycle regulation and apoptosis following exposure to proteasome inhibitors. *Cell Growth Differ.* 2000;11:239-246.
49. Schmidt-Karni O, Zupnick A, Castillo M, et al. p53 is localized to a sub-nucleolar compartment after proteasomal inhibition in an energy-dependent manner. *J Cell Sci.* 2008;121:4098-4105.
50. Khanna KK, Jackson SP. DNA double-strand breaks: signaling, repair and the cancer connection. *Nat Genet.* 2001;27:247-254.
51. Valenzano DR, Terzibasi E, Genade T, Cattaneo A, Domenici L, Cellerino A. Resveratrol prolongs lifespan and retards the onset of age-related markers in a short-lived vertebrate. *Curr Biol.* 2006;16:296-300.
52. Ahlander J, Bosco G. The Rb/E2F pathway and regulation of RNA processing. *Biochem Biophys Res Commun.* 2009;384:280-283.
53. Ding WX, Ni HM, Chen X, Yu J, Zhang L, Yin XM. A coordinated action of Bax, PUMA, and p53 promotes MG132-induced mitochondria activation and apoptosis in colon cancer cells. *Mol Cancer Ther.* 2007;6:1062-1069.
54. Del Priore LV, Kuo YH, Tezel TH. Age-related changes in human RPE cell density and apoptosis proportion in situ. *Invest Ophthalmol Vis Sci.* 2002;43:3312-3318.
55. Dunaief JL, Dentshev T, Ying GS, Milam AH. The role of apoptosis in age-related macular degeneration. *Arch Ophthalmol.* 2002;120:1435-1442.
56. Vuong L, Conley SM, Al-Ubaidi MR. Expression and role of p53 in the retina. *Invest Ophthalmol Vis Sci.* 2012;53:1362-1371.
57. Campisi J, Andersen JK, Kapahi P, Melov S. Cellular senescence: a link between cancer and age-related degenerative disease? *Semin Cancer Biol.* 2011;21:354-359.
58. Garcia-Cao I, Garcia-Cao M, Martin-Caballero J, et al. "Super-p53" mice exhibit enhanced DNA damage response, are tumor resistant and age normally. *EMBO J.* 2002;21:6225-6235.
59. Demidenko ZN, Korotchikina LG, Gudkov AV, Blagosklonny MV. Paradoxical suppression of cellular senescence by p53. *Proc Natl Acad Sci U S A.* 2010;107:9660-9664.
60. Wang AL, Lukas TJ, Yuan M, Neufeld AH. Age-related increase in mitochondrial DNA damage and loss of DNA repair capacity in the neural retina. *Neurobiol Aging.* 2010;31:2002-2010.
61. Bakkenist CJ, Kastan MB. DNA damage activates ATM through intermolecular autophosphorylation and dimer dissociation. *Nature.* 2003;421:499-506.
62. Tibbetts RS, Brumbaugh KM, Williams JM, et al. A role of ATR in the DNA damage-induced phosphorylation of p53. *Genes Dev.* 1999;13:152-157.
63. Olive PL. Endogenous DNA breaks: gammaH2AX and the role of telomeres. *Aging (Albany NY).* 2009;1:154-156.
64. Jaffe CA, Ameqrane I, Dansault A, et al. Sirt1 involvement in rd10 mouse retinal degeneration. *Invest Ophthalmol Vis Sci.* 2009;50:3562-3572.
65. Cheng HL, Mostoslavsky R, Saito S, et al. Developmental defects and p53 hyperacetylation in Sir2 homolog (SIRT1)-deficient mice. *Proc Natl Acad Sci U S A.* 2003;100:10794-10799.
66. Giordano A, Avantaggiati ML. p300 and CBP: partners for life and death. *J Cell Physiol.* 1999;181:218-230.
67. Dumitru R, Gama V, Fagan BM, et al. Human embryonic stem cells have constitutively active Bax the Golgi and are primed to undergo rapid apoptosis. *Mol Cell.* 2012;46:573-583.
68. Han J, Goldstein LA, Hou W, Gastman BR, Rabinowich H. Regulation of mitochondrial apoptotic events by p53-mediated disruption of complexes between antiapoptotic Bcl-2 members and Bim. *J Biol Chem.* 2010;285:22473-22483.
69. Peck B, Chen CY, Ho KK, et al. SIRT inhibitors induce cell death and p53 acetylation through targeting both SIRT1 and SIRT2. *Mol Cancer Ther.* 2010;9:844-855.
70. Brady CA, Attardi LD. p53 at a glance. *J Cell Sci.* 2010;123:2527-2532.
71. Kobet E, Zeng X, Zhu Y, Keller D, Lu H. Mdm2 inhibits p300-mediated p53 acetylation and activation by forming a ternary

- complex with the two proteins. *Proc Natl Acad Sci U S A*. 2000;97:12547-12552.
72. Kubota S, Kurihara T, Mochimaru H, et al. Prevention of ocular inflammation in endotoxin-induced uveitis with resveratrol by inhibiting oxidative damage and nuclear factor-kappaB activation. *Invest Ophthalmol Vis Sci*. 2009;50:3512-3519.
73. Uchiki T, Weikei KA, Jiao W, et al. Glycation-altered proteolysis as a pathobiologic mechanism that links dietary glycemic index, aging, and age-related disease (in nondiabetics). *Aging Cell*. 2012;11:1-13.
74. Bojarski C, Weiske J, Schoneberg T, et al. The specific fates of tight junction proteins in apoptotic epithelial cells. *J Cell Sci*. 2004;117:2097-2107.
75. Hwang SG, Lee HC, Trepel JB, Jeon BH. Anticancer-drug-induced apoptotic cell death in leukemia cells is associated with proteolysis of beta-catenin. *Leuk Res*. 2002;26:863-871.
76. Zhang H, Gao X, Yan Z, et al. Inhibiting caspase-3 activity blocks beta-catenin degradation after focal ischemia in rat. *Neuroreport*. 2008;19:821-824.